

Noise spectrum of quantum transport through quantum dots: a combined effect of non-Markovian and cotunneling processes

Jinshuang Jin,^{1,*} Wei-Min Zhang,^{2,†} Xin-Qi Li,³ and YiJing Yan⁴

¹ *Department of Physics, Hangzhou Normal University, Hangzhou 310036, China*

² *Department of Physics and Center for Quantum Information Science, National Cheng Kung University, Tainan 70101, Taiwan*

³ *Department of Physics, Beijing Normal University, Beijing 100875, China*

⁴ *Department of Chemistry, Hong Kong University of Science and Technology, Kowloon, Hong Kong*

(Dated: June 9, 2018)

Based on our recently developed quantum transport theory in term of an exact master equation, the corresponding particle-number resolved (n -resolved) master equation and the related shot noise spectrum formalism covering the full frequency range are constructed. We demonstrate that the noise spectra of transport current through single quantum dot and double quantum dots show characteristic steps and/or peak-dips in different tunneling frequency regimes through tuning the applied bias voltage and/or gate voltage at low temperatures. The peak-dips crossing the tunneling resonant frequencies is a combination effect of non-Markovian and cotunneling processes. These voltage-dependent tunneling resonance characteristics can be utilized to effectively modulate the internal Rabi resonance signature in the noise spectrum.

PACS numbers: 72.10.Bg; 05.40.-a

I. INTRODUCTION

Shot noise of non-equilibrium current fluctuations contains rich information beyond the average current.^{1,2} It has stimulated great interest in recent years both in theory and experiment.³⁻¹³ The evaluation of shot noise depends on the development of non-equilibrium quantum transport theory. Conventional approaches to quantum transport include the Landauer-Büttiker scattering matrix theory,^{1,14} the non-equilibrium Green's function formalism,^{15,16} and the real-time diagrammatic technique.^{17,18} Many interesting problems such as super- and sub-Poissonian noises and their origins have been addressed.^{1,6,19,20} However, most of the investigations focused only on the zero- or low-frequency regions. The evaluation of noise spectrum over the full frequency range is largely lacking and remains challenging with these approaches. Another commonly used method in quantum transport is the quantum master equation approach. In a certain sense it is simpler and more straightforward than the approaches mentioned above.⁷ It has the advantage of generality for different scattering processes being handled in a unified manner, even the transient dynamics under the time-dependent bias voltage.²¹⁻²³

Quantum transport theory based on master equation has been developed rapidly and studied extensively in recent years.^{3-8,13,24-26} However, most of work were based on a certain perturbative master equation description, which is valid mainly in Markovian dynamics dominated regime with sequential tunneling processes involving only one electron tunneling events at a time.^{3-8,13,24,25} Very recently, on the basis of Feynman-Vernon influence functional technique,²⁷ one of us has obtained an exact master equation for nanostructures,²⁸ from which we have also established an exact non-equilibrium quantum transport theory for noninteracting electronic systems.²³ This

new non-equilibrium quantum transport theory is applicable for arbitrary voltage, arbitrary temperature and arbitrary system-reservoir coupling strength. Quantum transport based on this exact treatment can deal with all the non-Markovian tunneling processes accompanied with not only sequential tunneling but also cotunneling involving two or more electron tunneling events at the same time.^{29,30}

In this paper, we will construct the corresponding master equation for the reduced density matrix conditioned on the electron number passed through the tunnel junction, i.e. the particle-number resolved (n -resolved) master equation. Together with the MacDonald's formula, we give the description for non-Markovian noise spectrum over the full frequency range. All relevant formulations will be summarized and developed in Sec. II together with the detailed numerical method presented in Appendix. This formalism is certainly applicable to arbitrary bias voltage, temperature and system-reservoir coupling strength for all the non-Markovian processes. In Sec. III, based on the present formulation, we study the quantum transport setup for the shot noise of current through two model systems. The first model is a single one-level quantum dot system, operated in the conventional sequential tunneling regime when only the average current is concerned. From the noise spectrum, however, we find that there emerge peak-dips in the noise spectrum as the temperature decreases. Another example is a coupled double quantum dots system, with one level in each dot. The resulting noise spectrum shows both the coherent Rabi resonance of the dots system and the external field-dependent tunneling characteristic resonant structure. We observe that the coherent Rabi resonance is insensitive to the temperature, while the external field-dependent tunneling resonant structure has the very interesting temperature-dependent phenomena. In partic-

ular, the external field-dependent tunneling resonance characteristics is manifested with either a peak-dip or a step at low temperature, depending on the corresponding tunneling regime defined by the applied bias and/or gate voltage. Consequently, by varying the applied voltage one can tune the tunneling resonance on top of the Rabi resonance, thus effectively modulate the coherent signature in noise spectrum. Finally, a summary is presented in Sec. IV.

II. n -RESOLVED MASTER EQUATION AND NOISE SPECTRUM

A. Exact master equation and transient transport current

Let us start with a brief outline of the recently developed exact master equation and the non-equilibrium quantum transport theory.^{23,28} The quantum transport studied with a nano-device consists of such as quantum dots interacting with the electron reservoirs (source and drain). The total Hamiltonian of the system has three parts: $H_T = H_S + H_B + H'$. The central system of quantum dots part assumes $H_S = \sum_{\mu} \epsilon_{\mu\mu} a_{\mu}^{\dagger} a_{\mu}$, where a_{μ}^{\dagger} (a_{μ}) is the creation (annihilation) operator of electron at the specified state of energy $\epsilon_{\mu\mu} \equiv \epsilon_{\mu}$, while the off-diagonal $\epsilon_{\mu\nu}$ is the hopping integral. The Hamiltonian of free-electron reservoirs reads $H_B = \sum_{\alpha k} \epsilon_{\alpha k} c_{\alpha k}^{\dagger} c_{\alpha k}$, with $c_{\alpha k}^{\dagger}$ being the creation operator for the electron in the reservoir $\alpha = L, R$. The system-reservoirs coupling for electron tunneling is given by

$$H' = \sum_{\alpha k \mu} V_{\alpha k \mu} a_{\mu}^{\dagger} c_{\alpha k} + \text{H.c.} \quad (1)$$

where $V_{\alpha k \mu}$ is the tunneling coefficient or the tunneling amplitude between the system and the reservoir α . The electron-electron interaction has been ignored here. Then the reduced density matrix of the central system $\rho(t) \equiv \text{tr}_B[\rho_T(t)]$, i.e., the trace of total density matrix over reservoirs degrees of freedom, is governed by the exact master equation^{23,28}

$$\begin{aligned} \dot{\rho}(t) = & -i[\tilde{H}_S(t), \rho(t)] - \sum_{\alpha \mu \nu} \tilde{\gamma}_{\alpha \mu \nu}(t) [a_{\mu}^{\dagger}, a_{\nu} \rho(t) + \rho(t) a_{\nu}] \\ & - \sum_{\alpha \mu \nu} \gamma_{\alpha \mu \nu}(t) \left(\frac{1}{2} a_{\mu}^{\dagger} a_{\nu} \rho(t) + \frac{1}{2} \rho(t) a_{\mu}^{\dagger} a_{\nu} - a_{\nu} \rho(t) a_{\mu}^{\dagger} \right). \end{aligned} \quad (2)$$

where the first term represents the Liouville equation (the unitary part) of the system with the renormalized Hamiltonian $\tilde{H}_S(t) = \sum_{\mu \nu} \tilde{\epsilon}_{\mu \nu} a_{\mu}^{\dagger} a_{\nu}$ and the renormalized energy levels $\tilde{\epsilon}(t) = \epsilon(t) - \frac{i}{2} \sum_{\alpha} [\kappa_{\alpha}(t) - \kappa_{\alpha}^{\dagger}(t)]$. The other two terms (the non-unitary part) in Eq. (2) describe the dissipation and decoherence dynamics of the system with

the time-dependent dissipation and fluctuation coefficients $\gamma_{\alpha}(t) \equiv \frac{1}{2} [\kappa_{\alpha}(t) + \kappa_{\alpha}^{\dagger}(t)]$ and $\tilde{\gamma}_{\alpha}(t) \equiv \lambda_{\alpha}(t) + \lambda_{\alpha}^{\dagger}(t)$, where $\kappa_{\alpha}(t)$ and $\lambda_{\alpha}(t)$ are given by,

$$\kappa_{\alpha}(t) = \int_{t_0}^t d\tau \mathbf{g}_{\alpha}(t, \tau) \mathbf{u}(\tau) [\mathbf{u}(t)]^{-1}, \quad (3a)$$

$$\lambda_{\alpha}(t) = \int_{t_0}^t d\tau \{ \mathbf{g}_{\alpha}(t, \tau) \mathbf{v}(\tau) - \mathbf{g}_{\alpha}(t, \tau) \bar{\mathbf{u}}(\tau) \} - \kappa_{\alpha}(t) \mathbf{v}(t). \quad (3b)$$

and $\mathbf{u}(\tau)$ and $\mathbf{v}(\tau)$ are indeed directly related to the Keldysh's non-equilibrium Green functions and they obey the following dissipation-fluctuation integrodifferential (Dyson) equations:^{23,28}

$$\dot{\mathbf{u}}(\tau) + i\epsilon(\tau) \mathbf{u}(\tau) + \sum_{\alpha} \int_{t_0}^{\tau} d\tau' \mathbf{g}_{\alpha}(\tau, \tau') \mathbf{u}(\tau') = 0, \quad (4a)$$

$$\begin{aligned} \dot{\mathbf{v}}(\tau) + i\epsilon(\tau) \mathbf{v}(\tau) + \sum_{\alpha} \int_{t_0}^{\tau} d\tau' \mathbf{g}_{\alpha}(\tau, \tau') \mathbf{v}(\tau') \\ = \sum_{\alpha} \int_{t_0}^t d\tau' \tilde{\mathbf{g}}_{\alpha}(\tau, \tau') \bar{\mathbf{u}}(\tau'), \end{aligned} \quad (4b)$$

subject to the boundary conditions $\mathbf{u}(t_0) = \mathbf{1}$, and $\mathbf{v}(t_0) = 0$. The integral kernels in the above equations, $\mathbf{g}_{\alpha}(\tau, \tau')$ and $\tilde{\mathbf{g}}_{\alpha}(\tau, \tau')$, are defined by $\mathbf{g}_{\alpha \mu \nu}(\tau, \tau') = \sum_k V_{\alpha k \mu} V_{\alpha k \nu}^* e^{-i\epsilon_{\alpha k}(\tau - \tau')}$ and $\tilde{\mathbf{g}}_{\alpha \mu \nu}(\tau, \tau') = \sum_k V_{\alpha k \mu} V_{\alpha k \nu}^* f_{\alpha}(\epsilon_{\alpha k}) e^{-i\epsilon_{\alpha k}(\tau - \tau')}$, which depict all the non-Markovian memory processes of electrons through the tunnelings between the dot system and the leads, and $f_{\alpha}(\epsilon_{\alpha k}) = 1/(e^{\beta \alpha (\epsilon_{\alpha k} - \mu_{\alpha})} - 1)$ is the Fermi distribution function of the lead α in the initial equilibrium state. Introducing the spectral density functions of the α -lead coupled with the dot system: $\mathbf{\Gamma}_{\alpha}(\omega) \equiv \{\Gamma_{\alpha \mu \nu}(\omega) = 2\pi \sum_k V_{\alpha k \mu} V_{\alpha k \nu}^* \delta(\omega - \epsilon_{\alpha k})\}$, the memory kernels are reduced to

$$\mathbf{g}_{\alpha}(\tau, \tau') = \int \frac{d\omega}{2\pi} \mathbf{\Gamma}_{\alpha}(\omega) e^{-i\omega(t - \tau)}, \quad (5a)$$

$$\tilde{\mathbf{g}}_{\alpha}(\tau, \tau') = \int \frac{d\omega}{2\pi} f_{\alpha}(\omega) \mathbf{\Gamma}_{\alpha}(\omega) e^{-i\omega(t - \tau)}. \quad (5b)$$

Through out this work, we have set $e = \hbar = 1$.

The transient current of the α -lead is obtained as²³

$$\begin{aligned} I_{\alpha}(t) = & -2\text{Re} \int_{t_0}^t d\tau \text{Tr} \left\{ \mathbf{g}_{\alpha}(t - \tau) \mathbf{v}(\tau) - \tilde{\mathbf{g}}_{\alpha}(t - \tau) \bar{\mathbf{u}}(\tau) \right. \\ & \left. + \mathbf{g}_{\alpha}(t, \tau) \mathbf{u}(\tau) \boldsymbol{\varrho}(t_0) \mathbf{u}^{\dagger}(t) \right\}, \end{aligned} \quad (6)$$

with $\bar{\mathbf{u}}(\tau) = \mathbf{u}^{\dagger}(t - \tau)$ and $\boldsymbol{\varrho}(t)$ being the single particle reduced density matrix, $\varrho_{\mu \nu}(t) \equiv \text{tr}_s [a_{\nu}^{\dagger} a_{\mu} \rho(t)]$, satisfying $\boldsymbol{\varrho}(t) = \mathbf{v}(t) + \mathbf{u}(t) \boldsymbol{\varrho}(t_0) \mathbf{u}^{\dagger}(t)$. The above current expression can easily recover the Landauer-Büttiker formula obtained by scattering approach and the Keldysh's non-equilibrium Green function formulation, as detailed in Ref. 23.

B. n -resolved quantum master equation

Before constructing the n -resolved master equation, we should point out that the master equation of Eq. (2) was derived exactly for noninteracting quantum dot systems so that all the electron tunneling processes in such systems, including sequential tunneling and cotunneling processes together with all the non-Markovian memory effects, are fully taken into account. For noninteracting systems, the cotunneling processes refer to the tunnelings involving two and more electrons through the junctions simultaneously. In the conventional master equation in terms of perturbation expansion, one may expect that the sequential tunneling and cotunneling processes should be described separately by one pair and two or more pairs of electron creation and annihilation operators, respectively, in the non-unitary part of the master equation. However, for noninteracting systems, the master equation derived from the perturbation expansion up to the second order of the tunneling coefficients, i.e. $V_{\alpha k \mu}$ in Eq. (1), has indeed the same operator structure as that of the exact master equation of Eq. (2).²⁸ The only difference between the second-order (2nd-order) perturbative master equation and the exact master equation is manifested in the determination of the dissipation and fluctuation coefficients in the corresponding master equations. In the exact master equation of Eq. (2), these dissipation and fluctuation coefficients, i.e., $\gamma_{\alpha\mu\nu}(t)$ and $\tilde{\gamma}_{\alpha\mu\nu}(t)$, are determined by the Green functions $\mathbf{u}(\tau)$ and $\mathbf{v}(\tau)$ which satisfy the exact dissipation-fluctuation integrodifferential equations of Eq. (4). The non-Markovian memory effect and the cotunneling processes described in the exact master equation are fully characterized by the non-local integral kernels in Eq. (4), i.e. the Dyson equations through the iteration to all orders of the tunneling coefficients. Truncating Eq. (4) to the 2nd-order perturbation of the tunneling coefficients, all these time-dependent dissipation and fluctuation coefficients are reduced to the coefficients in the 2nd-order perturbative

master equation that can be derived directly from the quantum Liouville equation in the perturbation expansion approach. Since the 2nd-order perturbative master equation can only describe the sequential tunneling and Markovian process, it indicates that the cotunneling processes and non-Markovian effect in noninteracting systems are fully determined by the time-dependent dissipation and fluctuation coefficients from the solution of Eq. (4), rather than the operator structure of the master equation. The operator structure of the 2nd-order perturbative master equation is exactly the same as that of the exact master equation for noninteracting systems. The detailed derivation of this connection between the exact master equation and the 2nd-order perturbative master equation has been given in Ref. 28.

Based on such a connection between the exact master equation and the 2nd-order perturbative master equation we just discussed above, we can construct the corresponding n -resolved master equation from Eq. (2) for the conditioned reduced density operator $\rho^{(n_\alpha)}$, from the n -resolved 2nd-order perturbative master equation that has been derived explicitly from the 2nd-order perturbative master equation.²⁵ $\rho^{(n_\alpha)}$ is conditioned on the registered number n_α of electrons having passed through the tunnel junction between the specified α -lead and the central dots system. As it has been shown in Ref. 25, the resulting n -resolved 2nd-order perturbative master equation only modifies the corresponding non-unitary operator structure of the 2nd-order perturbative master equation, namely, it replaces only the registered jump terms $a_\mu^\dagger \rho a_\nu$ and $a_\mu \rho a_\nu^\dagger$, associating with the specified α -lead in the master equation by $a_\mu^\dagger \rho^{(n_\alpha+1)} a_\nu$ and $a_\mu \rho^{(n_\alpha-1)} a_\nu^\dagger$, respectively. Other terms remain the same but for $\rho^{(n_\alpha)}$. Since the exact master equation for noninteracting systems has the same operator structure of the 2nd-order perturbative master equation, by analogy, we obtain the corresponding n -resolved master equation of the exact master equation of Eq. (2):

$$\begin{aligned} \dot{\rho}^{(n_\alpha)}(t) = & -i[\tilde{H}_S, \rho^{(n_\alpha)}(t)] - \sum_{\mu\nu} \tilde{\gamma}_{\mu\nu}(t) [a_\mu^\dagger a_\nu \rho^{(n_\alpha)}(t) - \rho^{(n_\alpha)}(t) a_\nu a_\mu^\dagger] - \sum_{\mu\nu} \gamma_{\mu\nu}(t) \{a_\mu^\dagger a_\nu, \rho^{(n_\alpha)}(t)\} \\ & + \sum_{\mu\nu} [\tilde{\gamma}_{\alpha'\mu\nu}(t) + 2\gamma_{\alpha'\mu\nu}(t)] a_\nu \rho^{(n_\alpha)}(t) a_\mu^\dagger - \tilde{\gamma}_{\alpha'\mu\nu}(t) a_\mu^\dagger \rho^{(n_\alpha)}(t) a_\nu \\ & + \sum_{\mu\nu} [\tilde{\gamma}_{\alpha\mu\nu}(t) + 2\gamma_{\alpha\mu\nu}(t)] a_\nu \rho^{(n_\alpha-1)}(t) a_\mu^\dagger - \sum_{\mu\nu} \tilde{\gamma}_{\alpha\mu\nu}(t) a_\mu^\dagger \rho^{(n_\alpha+1)}(t) a_\nu. \end{aligned} \quad (7)$$

for keeping track the number of electrons tunneling only through one specific lead, e.g., the α -lead with $\alpha' \neq \alpha$,

and

$$\begin{aligned}
\dot{\rho}^{(n_L, n_R)}(t) = & -i[\tilde{H}_S, \rho^{(n_L, n_R)}(t)] - \sum_{\mu\nu} \tilde{\gamma}_{\mu\nu} [a_\mu^\dagger a_\nu \rho^{(n_L, n_R)}(t) - \rho^{(n_L, n_R)}(t) a_\nu a_\mu^\dagger] \\
& - \sum_{\mu\nu} \gamma_{\mu\nu} \{a_\mu^\dagger a_\nu, \rho^{(n_L, n_R)}(t)\} \\
& + \sum_{\mu\nu} [(\tilde{\gamma}_{L\mu\nu} + 2\gamma_{L\mu\nu}) a_\nu \rho^{(n_L-1, n_R)}(t) a_\mu^\dagger - \tilde{\gamma}_{L\mu\nu} a_\mu^\dagger \rho^{(n_L+1, n_R)}(t) a_\nu] \\
& + \sum_{\mu\nu} (\tilde{\gamma}_{R\mu\nu} + 2\gamma_{R\mu\nu}) a_\nu \rho^{(n_L, n_R-1)}(t) a_\mu^\dagger - \sum_{\mu\nu} \tilde{\gamma}_{R\mu\nu} a_\mu^\dagger \rho^{(n_L, n_R+1)}(t) a_\nu, \tag{8}
\end{aligned}$$

for conditionally keeping track the number of electrons tunneling through both the right and the left leads. Here we omit the time index in the time-dependent coefficients and have also defined $\tilde{\gamma}_{\mu\nu} \equiv \sum_{\alpha=L,R} \tilde{\gamma}_{\alpha\mu\nu}$. Both the n -resolved master equations of Eq. (7) and Eq. (8) will be used to derive the noise spectrum of an individual lead and the cross-correlation noise spectrum.

The same as the connection between the exact master equation and the 2nd-order perturbative master equation discussed in the beginning of this subsection, the n -resolved master equation, Eq. (7) and Eq. (8), also has the same operator structure as that of the n -resolved 2nd-order perturbative master equation.²⁵ The only difference is the dissipation and fluctuation coefficients in these master equations. The dissipation and fluctuation coefficients in the n -resolved 2nd-order perturbative master equation involve only sequential tunneling process and the Markovian dynamics.²⁵ However, the time-dependent dissipation and fluctuation coefficients in Eq. (7) and Eq. (8) that are determined by the exact non-equilibrium Green functions of Eq. (4) for noninteracting systems have taken into account simultaneously the sequential tunneling and cotunneling processes, so does for the non-Markovian dynamics. One may ask why the states such as $\rho^{(n_\alpha \pm 2)}$, $\rho^{(n_L-1, n_R+1)}$ and $\rho^{(n_L+1, n_R-1)}$, etc. which are expected to be directly related to the cotunneling processes for the electron registered detector in the perturbative expansion do not occur in Eq. (7) and Eq. (8). This must be the same reason as in the case of the master equation itself. In terms of the perturbative expansion, the master equation up to the higher order contains the dissipation and fluctuation terms involving two and more pairs of electron operators sandwiching the reduced density matrix that describe the cotunneling processes. But the exact master equation does not contain such terms. This is because the cotunneling processes has been all switched into the dissipation and fluctuation coefficients determined by the exact Dyson equations. Although we have not provided a rigorous derivation of Eq. (7) and Eq. (8), it should be the same reason that the n -resolved master equation, Eq. (7) and Eq. (8), can maintain the simple operator form because the time-dependent dissipation and fluctuation coefficients determined by the exact nonequilibrium Green functions can

address all the sequential tunneling and cotunneling processes as the non-Markovian memory dynamics.

As a justification and also a self-consistent check, from the n -resolved master equation of Eq. (7) with the identity $\rho(t) = \sum_{n_\alpha} \rho^{(n_\alpha)}(t)$, we can easily reproduce the exact master equation of Eq. (2). The exact current expression of Eq. (6) can also be reproduced from the n -resolved master equation of Eq. (7) as follows. With the knowledge of $\rho^{(n_\alpha)}(t)$, the tunneling electrons distribution can be readily evaluated via $P(n_\alpha, t) = \text{Tr}_S \rho^{(n_\alpha)}(t)$. This is the key quantity for full counting statistics.^{24,31,32} The m^{th} -moment of transport is just $\langle n_\alpha^m(t) \rangle \equiv \sum_{n_\alpha} n_\alpha^m P(n_\alpha, t)$, from which all transport properties can be obtained. For instance, the measured current which is related to the rate of the first moment, is given by $I_\alpha(t) = -\frac{d}{dt} \langle n_\alpha(t) \rangle$. Using the n -resolved master equation of Eq. (7), it is also easy to reproduce the exact expression of the transient transport current of Eq. (6). The capability of recovering the exact master equation of Eq. (2) and the exact transport current formula of Eq. (6) from Eq. (7) ensures that the n -resolved master equations we constructed here is the current one for noninteracting systems. Thus the current-current correlation noise spectrum which is related to the 2nd-order cumulant can be directly evaluated now from Eq. (7) and Eq. (8), which will be presented in the following.

C. Noise spectrum expression

We consider now the current noise spectrum, $S(\omega) = \mathcal{F} \{ \langle \delta I(t) \delta I(0) \rangle_s \}$, i.e., the full Fourier transformation (denoted by \mathcal{F}) of the fluctuating current-current correlation function that is symmetrized. For the total circuit current $I(t) = aI_L(t) - bI_R(t)$, which is typically the measured quantity in most experiments,¹ with the coefficients satisfying $a + b = 1$ related to the symmetry of the transport setup (e.g., junction capacitances), the circuit noise spectrum is $S(\omega) = a^2 S_L(\omega) + b^2 S_R(\omega) - 2ab S_{LR}(\omega)$.^{1,4,7}

The noise spectrum at individual lead $\alpha = L$ or R is given by the MacDonald's formula, $S_\alpha(\omega) \equiv S_{\alpha\alpha}(\omega) = 2\omega \int_0^\infty dt \sin(\omega t) \frac{d}{dt} [\langle n_\alpha^2(t) \rangle - (\bar{I}_\alpha t)^2]$. With the help of

Eq. (7), the involved quantity $\langle n_\alpha^2(t) \rangle$ satisfies

$$\begin{aligned} \frac{d}{dt} \langle n_\alpha^2(t) \rangle &= 2 \operatorname{tr} [(\tilde{\gamma}_\alpha + \gamma_\alpha) \mathcal{N}_\alpha + \tilde{\gamma}_\alpha \bar{\mathcal{N}}_\alpha] \\ &\quad + \operatorname{tr} [(\tilde{\gamma}_\alpha + \gamma_\alpha) \boldsymbol{\rho} - \tilde{\gamma}_\alpha \bar{\boldsymbol{\rho}}], \end{aligned} \quad (9)$$

where $\bar{\boldsymbol{\rho}} = 1 - \boldsymbol{\rho}$ is the single hole particle reduced density matrix, while $\mathcal{N}_{\alpha\mu\nu} \equiv \operatorname{tr}_s[a_\nu^\dagger a_\mu \hat{N}^\alpha]$ and $\bar{\mathcal{N}}_{\alpha\mu\nu} \equiv \operatorname{tr}_s[a_\mu a_\nu^\dagger \hat{N}^\alpha]$ are related to the number operator $\hat{N}^\alpha(t) \equiv \sum_{n_\alpha} n_\alpha \rho^{(n_\alpha)}(t)$. It satisfies

$$\frac{d\hat{N}^\alpha}{dt} = \mathcal{M}\hat{N}^\alpha + \operatorname{tr} [(\tilde{\gamma}_\alpha + \gamma_\alpha) \boldsymbol{\rho}] + \operatorname{tr} [\tilde{\gamma}_\alpha \bar{\boldsymbol{\rho}}], \quad (10)$$

with \mathcal{M} being the generator of Eq. (2) that is recast as $\dot{\rho} = \mathcal{M}\rho$. The initial conditions to Eqs. (9) and (10) are the stationary states without the electron tunneling, i.e., $\hat{N}_\alpha(0) = 0$ and $\rho(0) = \rho^{\text{st}}$. We have

$$\begin{aligned} S_\alpha(\omega) &= 4\omega \operatorname{Im} \mathcal{L} \left\{ \operatorname{tr} [(\tilde{\gamma}_\alpha + \gamma_\alpha) \mathcal{N}_\alpha + \tilde{\gamma}_\alpha \bar{\mathcal{N}}_\alpha] \right\} \\ &\quad + 2 \operatorname{Re} \mathcal{L} \left\{ \operatorname{tr} [(\tilde{\gamma}_\alpha + \gamma_\alpha) \boldsymbol{\rho}^{\text{st}} - \tilde{\gamma}_\alpha \bar{\boldsymbol{\rho}}^{\text{st}}] \right\}, \end{aligned} \quad (11)$$

where $\mathcal{L}\{f(t)\} = \int_0^\infty dt e^{i\omega t} f(t)$ denotes the Laplace transformation.

The cross correlation noise spectrum is given by^{13,33,34} $S_{LR}(\omega) = \frac{1}{2} \mathcal{F} \{ \langle \delta I_L(t) \delta I_R(0) \rangle_s + \langle \delta I_R(t) \delta I_L(0) \rangle_s \} = 2\omega \int_0^\infty dt \sin(\omega t) \frac{d}{dt} [\langle N_L(t) N_R(t) \rangle - (\bar{I}t)^2]$, where $\langle N_L(t) N_R(t) \rangle = \operatorname{tr} \sum_{n_L n_R} n_L n_R \rho^{(n_L, n_R)}(t)$. Again, with the help of Eq. (8), we obtain

$$\begin{aligned} S_{LR}(\omega) &= 2\omega \operatorname{Im} \mathcal{L} \left\{ \operatorname{tr} [(\tilde{\gamma}_L + \gamma_L) \mathcal{N}_R + \tilde{\gamma}_L \bar{\mathcal{N}}_R] \right. \\ &\quad \left. + \operatorname{tr} [(\tilde{\gamma}_R + \gamma_R) \mathcal{N}_L + \tilde{\gamma}_R \bar{\mathcal{N}}_L] \right\}. \end{aligned} \quad (12)$$

We thus have completed the expressions of the current noise spectrum, i.e., Eq. (11) and Eq. (12), which are the main results of the present work. They can be further written in the compacted formalism as

$$\begin{aligned} S_{\alpha\alpha'}(\omega) &= 2\omega \operatorname{Im} \mathcal{L} \left\{ \operatorname{tr} [(\tilde{\gamma}_\alpha + \gamma_\alpha) \mathcal{N}_{\alpha'} + \tilde{\gamma}_\alpha \bar{\mathcal{N}}_{\alpha'}] \right. \\ &\quad \left. + \operatorname{tr} [(\tilde{\gamma}_{\alpha'} + \gamma_{\alpha'}) \mathcal{N}_\alpha + \tilde{\gamma}_{\alpha'} \bar{\mathcal{N}}_\alpha] \right\} \\ &\quad + 2\delta_{\alpha\alpha'} \operatorname{Re} \mathcal{L} \left\{ \operatorname{tr} [(\tilde{\gamma}_\alpha + \gamma_\alpha) \boldsymbol{\rho}^{\text{st}} - \tilde{\gamma}_\alpha \bar{\boldsymbol{\rho}}^{\text{st}}] \right\}. \end{aligned} \quad (13)$$

It describes both the sequential tunneling and cotunneling processes together with the non-Markovian memory effect involved in the time-dependent dissipation and fluctuation coefficients $\gamma_\alpha(t)$ and $\tilde{\gamma}_\alpha(t)$ that also determine the master equation of Eq. (2) and the n -resolved master equation of Eq. (7). We will evaluate explicitly the noise spectrum using Eq. (13) in the coming section with two widely adopted quantum transport model systems. Since the time-dependence dissipation and fluctuation coefficients are determined by the functions $\mathbf{u}(\tau)$ and $\mathbf{v}(\tau)$ which are governed by Eq. (4), the key to understand

the cotunneling processes and the non-Markovian effect in the transient transport current and the noise spectrum is to solve exactly the integrodifferential equations of Eq. (4). The detailed numerical method is presented in Appendix based on a parameterization scheme.

As it is shown in Ref. 28, $\mathbf{u}(\tau)$ and $\mathbf{v}(\tau)$ accounts for all orders in perturbative expansion. If one solves Eq. (4) up to the second-order of the system-reservoir couplings, the resulting master equation recovers the 2nd-order master equation in the perturbation theory that has been studied widely in the literature, see for examples Refs. 6,7,13. The usual Markovian approximation is obtained under both the wide band limit $\Gamma_\alpha(\omega) = \Gamma_\alpha$ with high temperature, which leads to $\mathbf{g}_\alpha(t - \tau) \rightarrow \frac{\Gamma_\alpha}{2} \delta(t - \tau)$ and $\tilde{\mathbf{g}}_\alpha(t - \tau) \rightarrow \frac{\Gamma_\alpha}{2} f_\alpha \delta(t - \tau)$. Then all the time-dependent coefficients in the master equation become constants, e.g., $\gamma_\alpha(t) = \Gamma_\alpha$ and $\tilde{\gamma}_\alpha(t) = -f_\alpha \Gamma_\alpha$, which recovers the n -resolved Markovian master equation in Ref. 35 and also reproduces the solution given in Ref. 31 for resonant-level model.

Usually one believes that in the wideband limit and the high bias voltage regime, the non-Markovian effect vanishes and the Markovian master equation works. However, the non-Markovian memory effect is very complicated, it relates to several factors together, such as the temperature, the bias voltage, the spectral bandwidth, and the system-reservoir coupling strength as details in Ref. 23 and in Appendix. In Ref. 23, we showed that in the WBL, the large bias voltage indeed weakens the non-Markovian effect, but does not lead to a complete Markovian limit. At this regime, the non-Markovian effect, which arise completely from the low temperature and/or strong system-reservoir coupling strength, may not be clearly manifested in the transport current itself and the reduced density matrix,²³ but it becomes significant in the noise spectrum of the current-current fluctuation,^{4,13} as shown in the next section.

III. NUMERICAL DEMONSTRATIONS

A. Single quantum dot system

For simplicity, we consider in this section the situation of an energy-independent spectral density of the leads, namely, the flat band of $\Gamma_\alpha(\omega) = \Gamma_\alpha$ and denote $\Gamma = \Gamma_L + \Gamma_R$. We set the symmetric junction capacitances as $a = b = 0.5$ and also the symmetric bias of $\mu_L = -\mu_R = eV/2$ in the following studies. Let us start with a single one-level dot model system, with $H_S = \varepsilon a^\dagger a$. The average current of this system can be evaluated as $\bar{I} = \Gamma_L \Gamma_R \int \frac{d\omega}{2\pi} \frac{f_L(\omega) - f_R(\omega)}{(\varepsilon - \omega)^2 + (\Gamma/2)^2}$. Despite of its simplicity, such a single quantum dot system has many interesting physical phenomena and has been widely used as a single electron transistor. Here we operate the system in the large voltage regime, $\mu_L > \varepsilon > \mu_R$, which is also considered as the conventional sequential tunneling

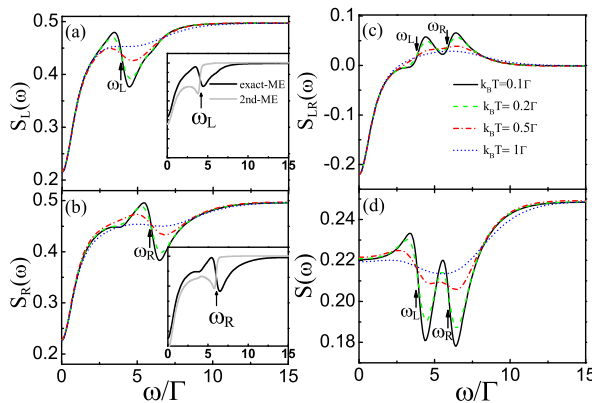


FIG. 1: Noise spectrum (in unit of $e^2\Gamma/\hbar$) for current transport through single quantum dot, where $\epsilon = \Gamma$, with $\Gamma_L = \Gamma_R = 0.5\Gamma$, under the bias of $V = 10\Gamma$ at the specified temperatures. The peak-dips crossing the tunneling resonance frequencies, $\omega_\alpha = |\epsilon - \mu_\alpha|$ with $\alpha = L$ and R , are indicated by arrows. The inserting figures in (a) and (b) give a comparison between the exact solution with the 2nd-order perturbation result at the temperature $k_B T = 0.1\Gamma$.

regime if the average current is concerned. However, we will see below that in this case a striking non-Markovian character, manifested by a peak-dip, will emerge in the current noise spectrum.

Figure 1 shows the current noise spectrums for auto-correlations [Fig. 1(a) and (b)], cross-correlation [Fig. 1(c)], and circuit current correlation [Fig. 1(d)], at different temperatures. In the low or high frequency region, the noise spectrum is nearly independent of temperature, despite of the fact that the stationary current increases as temperature decreases. In the large frequency regime, the noise spectrum at the individual lead $S_\alpha(\omega) \rightarrow \Gamma_\alpha$, while that of cross-lead $S_{LR}(\omega) \rightarrow 0$. More interestingly we observe that a peak-dip feature is developed in the noise spectrum of current auto- and cross-correlations, crossing each resonant frequency $\omega_\alpha = |\epsilon - \mu_\alpha|$ (indicated by an arrow in Fig. 1) as the temperature decreasing.

The above observations can be understood as follows. As the zero-frequency noise and also the stationary current are concerned, the transport system studied here with $\mu_L > \epsilon > \mu_R$ is dominated by sequential tunneling processes. In the high frequency ($\omega \gg |\epsilon - \mu_\alpha|$) region, we have $S_{LR}(\omega) \rightarrow 0$, due to the electron correlation between different leads is yet to be established. However, $S_\alpha(\omega) \rightarrow \Gamma_\alpha$ coming from the fact that the fluctuations arises mainly from the reservoir background. Therefore, we cannot find the system-associated structure in the noise spectrum at both limits. However, the shot noise over the full frequency range describes various tunnelings associated with energy emissions and absorptions at different detection frequency ω . Therefore it must manifest the energy structure dependence of the dot system through the applied bias voltage and temperature. As

one can see from Fig. 1, the noise spectrum at relative high temperature shows a smooth energy-structure dependence near the resonant frequency $\omega_\alpha = |\epsilon - \mu_\alpha|$. This result is consistent with that of Refs. 4 and 13, in which one used the second-order time-nonlocal master equation which contains very little memory when $k_B T > \Gamma$ and describes only the sequential tunneling process where the Markovian dynamics is dominated. However, non-Markovian dynamics should play an important role in the noise spectrum at low temperature ($k_B T \ll \Gamma$) where cotunneling processes should become significant, especially around the resonant frequency where the electron can dramatically tunnel forth and back between the leads and the dot near the Fermi surface of the leads. The observed peak-dip crossing the resonant frequency in $S_\alpha(\omega)$ [Fig. 1(a) and (b)] and $S_{LR}(\omega)$ [Fig. 1(c)] is indeed such a non-Markovian result as a combination of sequential tunneling and cotunneling processes at low temperature. In particular, the positive peak-dip feature in the cross-correlation fluctuations spectrum must come from the cross-lead cotunneling contribution.

The above peak-dips crossing the resonant frequencies in the noise spectrum have not been shown in the previous studies.^{4,6-8,12,13,24,36} This is because in Refs. 6-8, the Markovian treatment has been used, while Refs. 4 and 13 considered only the sequential tunneling process at relative high temperature with the 2nd-order master equation approach which is also Markovian dynamics dominated. Refs. 12 used Büttiker's scattering matrix approach which is exact at zero frequency but contains approximation that covers mainly the Markovian dynamics at finite frequency.^{14,37} To make a comparison, we calculate the noise spectrum with 2nd-order perturbation approximation at low temperature. The result is inserted in Fig. 1(a) and (b). It shows that the 2nd-order perturbation noise spectrum shows a dip only but not a peak-dip. As it is well-known the 2nd-order perturbation approximation is invalid at low temperature. Very recently, using the nonperturbative hierarchical equation of motion treatment,³⁸ this peak-dip feature in the noise spectrum is also observed. Fig. 1 also clearly shows that with the temperature increasing, the aforementioned non-Markovian effect, i.e. the peak-dips in the noise spectrum, is diminished. We thus conclude that the observed peak-dip feature in the noise spectrum is a non-Markovian memory effect through various tunneling processes, including both the sequential tunneling and cotunneling events.

B. Double quantum dots

Consider now the transient transport through a system of two coupled quantum dots, described by $H_S = \sum_{\mu=l,r} \epsilon_\mu d_\mu^\dagger d_\mu + \Omega(d_l^\dagger d_r + d_r^\dagger d_l)$. This system has been studied widely as a charge qubit^{7,10,28,36} and has also been proposed as an alternative detector of a charge qubit.³⁹ The intrinsic coherent Rabi frequency Δ is the

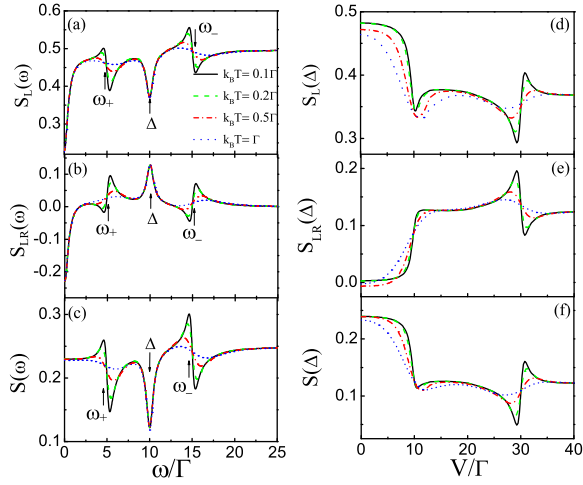


FIG. 2: Shot noise (in unit of $e^2\Gamma/\hbar$) of a double-dots system, where $\varepsilon_l = \varepsilon_r = 0$ and $\Omega = 5\Gamma$, with $\Gamma_L = \Gamma_R = 0.5\Gamma$ at the specified temperatures. Left panels: The noise spectrum as a function of frequency, under the bias voltage $eV = 20\Gamma$. The tunneling resonances of the peak-dip characteristics occurs at $\omega_{\pm} = |\varepsilon_{\pm} - \mu_{\alpha}| = 5\Gamma$ and 15Γ and the Rabi resonance at $\Delta = 10\Gamma$, indicated by the arrows individually. Right panels: The shot noise at the Rabi frequency $\omega = \Delta$ as function of bias voltage. The double-resonance $\omega = \Delta = |\varepsilon_{\pm} - \mu_{\alpha}|$ occurs at both $eV = 10\Gamma$ and $eV = 30\Gamma$. The former satisfies also the resonant transport conditions $\mu_L = \varepsilon_+$ and $\mu_R = \varepsilon_-$, but the latter is of $\mu_L > \varepsilon_{\pm} > \mu_R$.

energy difference between eigenstates (ε_{\pm}), e.g., $\Delta = \varepsilon_+ - \varepsilon_- = 2\Omega$ for the degenerate double-dots system considered for demonstrations. It is known^{7,36} that the Rabi coherence of the central system shows a dip at $\omega = \Delta$ in the auto-correlation noise spectrum $S_{\alpha}(\omega)$, as can be seen in Fig.2(a). But, it appears a peak in the cross-correlation noise spectrum $S_{LR}(\omega)$, as shown in Fig.2(b), while remains a dip in the total circuit noise spectrum, for symmetric junction capacitances, as depicted in Fig.2(c). The above Rabi coherence signatures are nearly independent of the temperature. Physically, the Rabi coherence is intrinsic. Therefore, it can be extracted even in the weak system-reservoir coupling regime, where the 2nd-order master equation is applicable.^{7,36} Besides the coherent signals of Rabi frequency in Fig.2(a)-(c) where $\mu_L > \varepsilon_{\pm} > \mu_R$, the expected peak-dips of non-Markovian characteristics occur at tunneling resonance of $\omega_{\pm} = |\varepsilon_{\pm} - \mu_{\alpha}|$ at low temperature. As temperature increases, this peak-dip feature is diminished, just the same as that in the single quantum dot case described earlier.

Figure 2(d)-(f) depict the noise spectrum at Rabi resonance $\omega = \Delta$ versus the applied bias voltage V that monitors the tunneling resonance of $\omega = |\varepsilon_{\pm} - \mu_{\alpha}|$. The double-resonance of $\omega = \Delta = |\varepsilon_{\pm} - \mu_{\alpha}|$ occurs at $V = 10\Gamma$ and $V = 30\Gamma$ for the present system in study. Apparently, the bias voltage dependence of the noise $S(\Delta)$ at Rabi frequency is changed dramatically

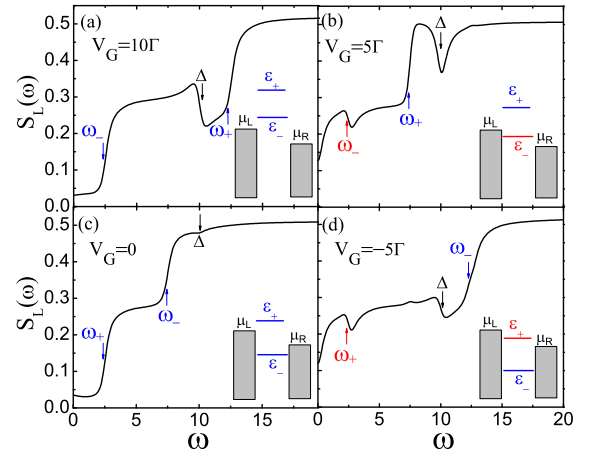


FIG. 3: Frequency-dependent noise spectrum of the left lead for the double-dots transport system with different tunneling regimes through gate voltage V_G , i.e., $\varepsilon_l = \varepsilon_r = V_G$, at low temperature $k_B T = 0.1\Gamma$ with the applied bias voltage $eV = 5\Gamma$. The other parameters are the same as in Fig. 2.

at low temperature, especially at tunneling resonance, as an expected non-Markovian effect. In particular, at $V = 30\Gamma$, both the two dot levels lie within the applied bias window, i.e., $\mu_L > \varepsilon_{\pm} > \mu_R$. The resulting peak-dip tunneling resonance shows up clearly in Fig. 2(d)-(f). The behavior of $S(\omega = \Delta)$ around $V = 10\Gamma$ is an interplay between the Rabi resonance and the lead-dot tunneling resonance.

The frequency-dependent noise spectra demonstrated in Fig.1 and Fig.2(a)-(c) are operated in the so-called large bias region of $\mu_L > \varepsilon_{\pm} > \mu_R$, where the tunneling resonance shows the peak-dip feature at low temperature, as a combination effect of the sequential tunneling and cotunneling events. Since the Rabi resonance spectral profile does not depend on the applied gate voltage for its overall intensity, we shall also examine the tunneling resonance behavior for different set up of the applied gate voltage to the dot energy levels. Without loss the generality, we take a fixed bias voltage, say $V = 5\Gamma$, and apply several different gate voltages to the dot levels to achieve different tunneling scenarios. The results are summarized in Fig. 3. Fig. 3(a) and (c) describe the case of both the two dot levels lying outside the bias voltage window. The corresponding tunneling resonance shows only with a step shape. In contrast, if one of the dot levels, i.e., the level ε_- and ε_+ in Fig. 3(b) and (d), respectively, lies inside the the bias voltage window, the corresponding tunneling resonance spectrum generates a peak-dip. As it has been understand, for the dot level lying outside the bias voltage window (i.e. either $\varepsilon > \mu_{L,R}$ or $\varepsilon < \mu_{L,R}$), the sequential tunneling through this level is largely suppressed and the transport is dominated by cotunneling events. So the cotunneling transport alone only shows a step near the resonance frequency. The peak-dip occurs only for $\mu_L > \varepsilon > \mu_R$ at low temperature, where both the sequential tunneling and cotunneling participate in

the non-Markovian dynamics.

IV. SUMMARY

In summary, based on the exact master equation for nonequilibrium transport, we constructed the corresponding particle-number resolved master equation, from which we have also established the formalism for the noise spectrum in the full frequency range. This new formalism is applicable to arbitrary bias voltage, temperature and system-reservoir coupling strength for all the non-Markovian processes in various nanoelectronic systems where the electron-electron interaction has been ignored. We applied this formalism to two widely studied transport model systems, i.e, electron transport through single quantum dot with a resonant level and double coupled quantum dots containing one energy level in each dot contacted the electron reservoirs, respectively. We showed different tunneling characteristics in the noise spectrum in both the large and small bias voltage regime at different temperature. In particular, we found peak-dips in the noise spectrum crossing the tunneling resonant frequencies which are defined individually by the energy difference between the applied chemical potentials and the dots energy levels. This peak-dip feature has not been observed in previous theoretical works. The characteristic peak-dip in the current noise spectra is a non-Markovian effect at low temperature involving both sequential tunneling and cotunneling. As the temperature increasing ($k_B T > \Gamma$), peak-dip profile in the noise spectrum is diminished. In contrast with the aforementioned external bias voltage regulated resonant characteristics, the internal coherent Rabi oscillation signal in the double dot system is rather independent of temperature. The coherent Rabi oscillation results in just a normal dip profile in the auto-correlation noise spectrum but a peak in the cross-correlation spectrum. We expect that these characteristics in the current noise spectra we found here would be tested in experiments or in other theoretical calculations.

We should also point out that the characteristic structure showing peak-dips in the noise spectrum may be changed after the electron-electron interaction is taken into account. More interesting phenomena in the noise spectrum should be expected in the interacting systems at low temperature. A closed formulation for the exact master equation of the reduced density matrix and the exact calculation of noise spectrum with the consideration of Coulomb interaction is not obvious. However, the present formalism is easy to be extended for including the Coulomb interaction with respect to the saddle point approximation⁴⁰ or loop expansion,⁴¹ where the Coulomb interaction can be treated self-consistently in generalizing integrodifferential equations of motion Eq. (4), or by means of Hierarchical equation of motion approach.²² The work along this line is in progress.

Acknowledgments

Support from NNSF China (10904029 and 10905014) and ZJNSF China (Y6090345), the NSC (NSC-99-2112-M-006-008-MY3) and National Center for Theoretical Science of Taiwan, and also UGC (AOE/P-04/08-2) and RGC (604709) of Hong Kong SAR Government is acknowledged.

Appendix: Numerical method

As mentioned in Sec. II C, the key to the practical calculation of the noise spectrum as well as the reduced density matrix Eq. (2) and current in Eq. (6) in the present formalism relies on how to solve the integrodifferential equations of Eq. (4), which contain all the non-Markovian memory effects of the central system interacting with its environment. In general, it is not possible to analytically solve Eq. (4) but the numerical solution of such integrodifferential equation is also very difficult due to the non-Markovian memory kernels. Here, in terms of a parameterized scheme,^{22,42} we develop a numerical method in terms of a closed set of coupled differential equations of motion for solving $\mathbf{u}(t)$ and $\mathbf{v}(t)$ to overcome the difficulties in the direct numerical calculation of the integrodifferential equations.

For the sake of generality, we start with the energy dependence spectral density as a Lorentzian-type form centered at ϵ_α .^{22,28,43}

$$\Gamma_\alpha(\omega) = \frac{\Gamma_\alpha W_\alpha^2}{(\omega - \epsilon_\alpha)^2 + W_\alpha^2}, \quad (14)$$

where Γ_α describes the coupling strength and W_α is the line width of the source (drain) reservoir with $\alpha = L(R)$. Obviously the wide band limit (flat band), $\Gamma_\alpha(\omega) = \Gamma_\alpha$, is achieved by simply letting $W_\alpha \rightarrow \infty$. In terms of Eq. (5), the non-local time correlation functions can be parameterized as^{22,23}

$$\mathbf{g}_\alpha(t, \tau) = \frac{\Gamma_\alpha W_\alpha}{2} e^{-\gamma_{\alpha 0}(t-\tau)}, \quad (15a)$$

$$\tilde{\mathbf{g}}_\alpha(t, \tau) = \sum_{m=0}^M \boldsymbol{\eta}_{\alpha m} e^{-\gamma_{\alpha m}(t-\tau)} \equiv \sum_{m=0}^M \tilde{\mathbf{g}}_{\alpha m}(t - \tau), \quad (15b)$$

with $\tilde{\mathbf{g}}_{\alpha m}(t - \tau) \equiv \boldsymbol{\eta}_{\alpha m} e^{-\gamma_{\alpha m}(t-\tau)}$. The first term in $\tilde{\mathbf{g}}_\alpha(t - \tau)$ with $m = 0$ arises from the pole of the spectral density function, with

$$\eta_{\alpha 0} = \frac{\Gamma_\alpha W_\alpha / 2}{1 + e^{-i\beta_\alpha(\gamma_{\alpha 0} - i\mu_\alpha)}}, \quad \gamma_{\alpha 0} = W_\alpha + i\epsilon_\alpha. \quad (16)$$

The other terms with $m > 0$ ($M \rightarrow \infty$ in principle) arise from the Matsubara poles, where the relevant parameters

are explicitly given as

$$\boldsymbol{\eta}_{\alpha m} = \frac{i}{\beta_\alpha} \boldsymbol{\Gamma}_\alpha(-i\gamma_{\alpha m}), \quad m = 1, \dots, \infty; \quad (17a)$$

$$\gamma_{\alpha m} = \frac{(2m-1)\pi}{\beta_\alpha} + i\mu_\alpha. \quad (17b)$$

The above parameterization is based on the Matsubara frequencies decomposition of Fermi distribution. An alternative efficient parameter scheme proposed in Ref. ⁴⁴ is Padé spectrum decomposition for its convergence significantly faster than other schemes at all temperatures. The resulting formalisms of Eq. (15) are unchanged, but the coefficients for $m > 0$ in $\tilde{\mathbf{g}}(t, \tau)$ are modified accordingly.⁴⁴ Here, following the procedure in Refs. 22,45 with the above parameterized scheme, we will present a numerical method in terms of a closed set of coupled differential equations of motion, instead of the integrodifferential equation of Eq. (4a), to solve the time-dependent transport current and the noise spectrum.

Introducing a new function $\mathbf{g}_\alpha^u(t) \equiv \int_{t_0}^t d\tau \mathbf{g}_\alpha(t, \tau) \mathbf{u}(\tau)$ which satisfies the following equation

$$\dot{\mathbf{g}}_\alpha^u(t) = \mathbf{g}_\alpha(0) \mathbf{u}(t) - \gamma_{\alpha 0} \mathbf{g}_\alpha^u(t), \quad (18)$$

with $\mathbf{g}_\alpha(0) = W_\alpha \boldsymbol{\Gamma}_\alpha / 2$, then Eq. (4a) is reduced to

$$\dot{\mathbf{u}}(t) = -i\epsilon(t) \mathbf{u}(t) - \sum_\alpha \mathbf{g}_\alpha^u(t). \quad (19)$$

In other words, the integrodifferential equation of Eq. (4a) is transformed into a coupled pure differential equations of Eq. (18) and Eq. (19), from which it is rather easy to obtain the time-dependent solution of $\mathbf{u}(t)$ and $\mathbf{g}_\alpha^u(t)$. On the other hand, the formal solution of Eq. (4b) is

$$\mathbf{v}(\tau, t) = \sum_\alpha \int_{t_0}^\tau d\tau_1 \int_{t_0}^\tau d\tau_2 \mathbf{u}(\tau, \tau_1) \tilde{\mathbf{g}}_\alpha(\tau_1, \tau_2) \mathbf{u}^\dagger(t, \tau_2), \quad (20)$$

from which we have

$$\mathbf{v}(t) \equiv \mathbf{v}(t, t) = \sum_\alpha \int_{t_0}^t d\tau_1 \int_{t_0}^t d\tau_2 \mathbf{u}(t, \tau_1) \tilde{\mathbf{g}}_\alpha(\tau_1, \tau_2) \mathbf{u}^\dagger(t, \tau_2). \quad (21)$$

Its time derivation is

$$\dot{\mathbf{v}}(t) = -i[\epsilon(t), \mathbf{v}(t)] - \sum_\alpha [\mathcal{I}_\alpha(t) + \text{H.c.}] \quad (22)$$

with $\mathcal{I}_\alpha(t) = \mathcal{K}_\alpha(t) + \mathcal{Q}_\alpha(t)$, where

$$\mathcal{K}_\alpha(t) \equiv \int_{t_0}^t d\tau \mathbf{g}_\alpha(t, \tau) \mathbf{v}(\tau, t), \quad (23a)$$

$$\mathcal{Q}_\alpha(t) \equiv - \int_{t_0}^t d\tau \tilde{\mathbf{g}}_\alpha(t, \tau) \mathbf{u}^\dagger(\tau, t) = \sum_{m=0}^M \mathcal{Q}_{\alpha m}(t). \quad (23b)$$

The second identity in Eq. (23b) is based on the parameterization scheme of $\tilde{\mathbf{g}}_\alpha(t, \tau)$ given by Eq. (15b), which leads to

$$\mathcal{Q}_{\alpha m}(t) = - \int_{t_0}^t d\tau \tilde{\mathbf{g}}_{\alpha m}(t, \tau) \mathbf{u}^\dagger(\tau, t), \quad (24)$$

Furthermore, by introducing new functions

$$\mathcal{C}_{\alpha\alpha'm}(t) \equiv \int_{t_0}^t d\tau \int_{t_0}^\tau d\tau_1 \mathbf{g}_\alpha(t, \tau) \mathbf{u}(\tau, \tau_1) \tilde{\mathbf{g}}_{\alpha'm}(\tau_1, t), \quad (25a)$$

$$\mathcal{D}_{\alpha\alpha'}(t) \equiv \int_{t_0}^t d\tau \int_{t_0}^\tau d\tau_1 \mathbf{g}_\alpha(t, \tau) \mathbf{v}(\tau, \tau_1) \mathbf{g}_{\alpha'}(\tau_1, t), \quad (25b)$$

we can find the following coupled differential equations:

$$\begin{aligned} \dot{\mathcal{K}}_\alpha(t) &= \mathcal{K}_\alpha(t)[i\epsilon(t) - \gamma_{\alpha 0}] + \mathbf{g}_\alpha(0) \mathbf{v}(t) \\ &\quad + \sum_{\alpha'm} [\mathcal{C}_{\alpha\alpha'm}(t) - \mathcal{D}_{\alpha\alpha'}(t)], \end{aligned} \quad (26a)$$

$$\dot{\mathcal{Q}}_{\alpha m}(t) = \mathcal{Q}_{\alpha m}(t)[i\epsilon(t) - \gamma_{\alpha m}] - \boldsymbol{\eta}_{\alpha m} + \sum_{\alpha'} \mathcal{C}_{\alpha'\alpha m}^\dagger(t), \quad (26b)$$

$$\dot{\mathcal{C}}_{\alpha\alpha'm}(t) = -\mathbf{g}_\alpha(0) \mathcal{Q}_{\alpha'm}^\dagger(t) - [\gamma_{\alpha 0}(t) + \gamma_{\alpha'm}^*(t)] \mathcal{C}_{\alpha\alpha'm}(t), \quad (26c)$$

$$\begin{aligned} \dot{\mathcal{D}}_{\alpha\alpha'}(t) &= \mathbf{g}_\alpha(0) \mathcal{K}_{\alpha'}^\dagger(t) + \mathcal{K}_\alpha(t) \mathbf{g}_{\alpha'}(0) \\ &\quad - [\gamma_{\alpha 0}(t) + \gamma_{\alpha'0}^*(t)] \mathcal{D}_{\alpha\alpha'}(t). \end{aligned} \quad (26d)$$

Solving numerically the coupled pure differential equation of Eq. (26) together with Eq. (22), we thus have the solution of $\mathbf{v}(t)$ and $\mathcal{I}_\alpha(t)$ without directly calculating the multi-integrals in Eq. (20). Consequently, all the time-dependent coefficients in the transient current of Eq. (6), the master equation of Eq. (2) and the n -resolved master equation of Eq. (7), as well as the frequency-dependent noise spectrum of Eq. (13) can be easily obtained through the relations $\boldsymbol{\kappa}_\alpha(t) = \mathbf{g}_\alpha^u(t) [\mathbf{u}(t)]^{-1}$ and $\boldsymbol{\lambda}_\alpha(t) = \mathcal{I}_\alpha(t) - \boldsymbol{\kappa}_\alpha(t) \mathbf{v}(t)$. This numerical method largely simplifies the numerical difficulties in solving the integrodifferential equations of Eq. (4) which involve very complicated non-Markovian memory kernels.

In the wideband limit $W_\alpha \rightarrow \infty$, the numerical calculation can be largely simplified. Explicitly, the temperature-independent memory kernel of Eq. (15a) is reduced to a delta function given by $\mathbf{g}(t, \tau) = \frac{\boldsymbol{\Gamma}_\alpha}{2} \delta(t - \tau)$. For the temperature-dependent memory kernel in Eq. (15b), the first term ($m = 0$) is also reduced to a delta function but the other terms ($m \geq 1$) are apparently changed not too much:

$$\begin{aligned} \tilde{\mathbf{g}}_\alpha(t - \tau) &\rightarrow \frac{\boldsymbol{\Gamma}_\alpha}{2(1 + e^{-i\beta_\alpha W_\alpha})} \delta(t - \tau) \\ &\quad + \frac{i}{\beta_\alpha} \boldsymbol{\Gamma}_\alpha \sum_{m=1}^M e^{-\gamma_{\alpha m}(t - \tau)}. \end{aligned} \quad (27)$$

Thus the non-Markovian effect in the wideband limit is determined by the temperature together with the bias

voltage and the system-reservoir coupling. If we take further a high temperature limit $\beta_\alpha \rightarrow 0$, the summation term in Eq.(27) will also be reduced to a delta function of $t - \tau$. Then no any memory effect remains, and a true Markov limit is reached at high temperature limit. In the practical numerical calculation, we keep the temperature-dependent memory kernel with the expression of Eq.(15b) and the WBL is taken by setting $W_\alpha \geq 100\Gamma$.^{23,46} The equations of the m -related quantities, such as $\mathbf{v}(t)$, $\mathcal{Q}_{\alpha m}(t)$, and $\mathcal{C}_{\alpha\alpha'm}(t)$ given by Eq.(22), Eq.(26b) and Eq.(26c), respectively, are thus

not changed. The other equations can be simplified as follows. The equation of Eq.(19) is recast to

$$\dot{\mathbf{u}}(t) = -i\epsilon(t)\mathbf{u}(t) - \frac{\Gamma}{2}\mathbf{u}(t), \quad (28)$$

and Eq.(18) is not needed. Also, we can simply solve Eq.(23a) and Eq.(25b) with the results $\mathcal{K}_\alpha = \Gamma_\alpha \mathbf{v}(t)/2$ and $\mathcal{D}_{\alpha\alpha'}(t) = \Gamma_\alpha \mathbf{v}(t)\Gamma_{\alpha'}/4$ but Eq.(26a) and Eq.(26d) are also no longer used.

-
- * Electronic address: hznu.jin@gmail.com
† Electronic address: wzhang@mail.ncku.edu.tw
- ¹ Y. M. Blanter and M. Büttiker, Phys. Rep. **336**, 1 (2000).
 - ² *Quantum Noise in Mesoscopic Physics* (Kluwer, Dordrecht, 2003), edited by Y. V. Nazarov.
 - ³ H. B. Sun and G. J. Milburn, Phys. Rev. B **59**, 10748 (1999).
 - ⁴ H.-A. Engel and D. Loss, Phys. Rev. Lett. **93**, 136602 (2004).
 - ⁵ O. Entin-Wohlman, Y. Imry, S. A. Gurvitz, and A. Aharony, Phys. Rev. B **75**, 193308 (2007).
 - ⁶ C. Flindt, T. Novotny, A. Braggio, M. Sassetti, and A.-P. Jauho, Phys. Rev. Lett. **100**, 150601 (2008).
 - ⁷ J. Y. Luo, X. Q. Li, and Y. J. Yan, Phys. Rev. B **76**, 085325 (2007).
 - ⁸ B. Dong, X. L. Lei, and N. J. M. Horing, J. Appl. Phys. **104**, 033532 (2008).
 - ⁹ S. S. Safonov, A. K. Savchenko, D. A. Bagrets, O. N. Jouravlev, Y. V. Nazarov, E. H. Linfield, and D. A. Ritchie, Phys. Rev. Lett. **91**, 136801 (2003).
 - ¹⁰ G. Kießlich, E. Schöll, T. Brandes, F. Hohls, and R. J. Haug, Phys. Rev. Lett. **99**, 206602 (2007).
 - ¹¹ Y. M. Zhang, L. DiCarlo, D. T. McClure, M. Yamamoto, S. Tarucha, C. M. Marcus, M. P. Hanson, and A. C. Gossard, Phys. Rev. Lett. **99**, 036603 (2007).
 - ¹² E. A. Rothstein, O. Entin-Wohlman, and A. Aharony, Phys. Rev. B **79**, 075307 (2009).
 - ¹³ J. S. Jin, X. Q. Li, M. Luo, and Y. J. Yan, J. Appl. Phys. **109**, 053704 (2011).
 - ¹⁴ M. Büttiker, Physica B **175**, 199 (1991).
 - ¹⁵ L. Y. Chen and C. S. Ting, Phys. Rev. B **43**, 4534 (1991).
 - ¹⁶ K.-M. Hung and G. Y. Wu, Phys. Rev. B **48**, 14687 (1993).
 - ¹⁷ M. Braun, J. König, and J. Martinek, Phys. Rev. B **74**, 075328 (2006).
 - ¹⁸ H. Schoeller and G. Schön, Phys. Rev. B **50**, 18436 (1994).
 - ¹⁹ A. Thielmann, M. H. Hettler, J. König, and G. Schön, Phys. Rev. B **71**, 045341 (2005).
 - ²⁰ J. H. Davies, P. Hylgaard, S. Hershfield, and J. W. Wilkins, Phys. Rev. B **46**, 9620 (1992).
 - ²¹ X. Q. Li and Y. J. Yan, Phys. Rev. B **75**, 075114 (2007).
 - ²² J. S. Jin, X. Zheng, and Y. J. Yan, J. Chem. Phys. **128**, 234703 (2008).
 - ²³ J. S. Jin, M. W.-Y. Tu, W.-M. Zhang, and Y. J. Yan, New J. Phys. **12**, 083013 (2010).
 - ²⁴ G. Kießlich, P. Samuelsson, A. Wacker, and E. Schöll, Phys. Rev. B **73**, 033312 (2006).
 - ²⁵ X. Q. Li, J. Y. Luo, Y. G. Yang, P. Cui, and Y. J. Yan, Phys. Rev. B **71**, 205304 (2005).
 - ²⁶ A. Braggio, J. König, and R. Fazio, Phys. Rev. Lett. **96**, 026805 (2006).
 - ²⁷ R. P. Feynman and F. L. Vernon, Jr., Ann. Phys. **24**, 118 (1963).
 - ²⁸ M. W. Y. Tu and W.-M. Zhang, Phys. Rev. B **78**, 235311 (2008).
 - ²⁹ S. D. Franceschi, S. Sasaki, J. M. Elzerman, W. G. van der Wiel, S. Tarucha, and L. P. Kouwenhoven, Phys. Rev. Lett. **86**, 878 (2001).
 - ³⁰ D. Averin and Y. Nazarov, in *Single Charge Tunneling: Coulomb Blockade Phenomena in Nanostructures*, edited by H. Grabert and M. H. Devoret (Plenum Press and NATO Scientific Affairs Division, New York, 1992), p. 217.
 - ³¹ D. A. Bagrets and Y. V. Nazarov, Phys. Rev. B **67**, 085316 (2003).
 - ³² S. Gustavsson, R. Leturcq, B. Simovic, R. Schleser, T. Ihn, P. Studerus, K. Ensslin, D. C. Driscoll, and A. C. Gossard, Phys. Rev. Lett. **96**, 076605 (2006).
 - ³³ B. Wang, J. Wang, and H. Guo, Phys. Rev. B **69**, 153301 (2004).
 - ³⁴ B. Dong, H. L. Cui, and X. L. Lei, Phys. Rev. Lett. **94**, 066601 (2005).
 - ³⁵ S. A. Gurvitz and Y. S. Prager, Phys. Rev. B **53**, 15932 (1996).
 - ³⁶ R. Aguado and T. Brandes, Phys. Rev. Lett. **92**, 206601 (2004).
 - ³⁷ M. Büttiker, Phys. Rev. B **45**, 3807 (1992).
 - ³⁸ S. K. Wang, *et. al*, in preparation. Based on the Hierarchical equation of motion approach,²² we can establish the hierarchically exact n -resolved master equation, the resulted noise spectrum has also shown the peak-dip feature in the same frequency regime as studied in the present work.
 - ³⁹ T. Gilad and S. A. Gurvitz, Phys. Rev. Lett. **97**, 116806 (2006).
 - ⁴⁰ A. Kamenev and A. Andreev, Phys. Rev. B **60**, 2218 (1999).
 - ⁴¹ W.-M. Zhang and L. Wilets, Phys. Rev. C **45**, 1900 (1992).
 - ⁴² A. Croy and U. Saalman, Phys. Rev. B **80**, 245311 (2009).
 - ⁴³ J. Maciejko, J. Wang, and H. Guo, Phys. Rev. B **74**, 085324 (2006).
 - ⁴⁴ J. Hu, R. X. Xu, and Y. J. Yan, J. Chem. Phys. **133**, 101106 (2010).
 - ⁴⁵ A. Croy and U. Saalman, Phys. Rev. B **80**, 245311 (2009).
 - ⁴⁶ J. Wang, B. Wang, and H. Guo, Phys. Rev. B **75**, 155336 (2007).